Quaternary Science Reviews 131 (2016) 148–156

Contents lists available at ScienceDirect

Quaternary Science Reviews

journal homepage: www.elsevier.com/locate/quascirev

Solar forcing as an important trigger for West Greenland sea-ice variability over the last millennium

Longbin Sha [a, b, *], Hui Jiang [a, c], Marit-Solveig Seidenkrantz [d], Raimund Muscheler [e], Xu Zhang [f], Mads Faurschou Knudsen [d], Jesper Olsen [g], Karen Luise Knudsen [d], Weiguo Zhang [c]

[a] Key Laboratory of Geographic Information Science, East China Normal University, 200062 Shanghai, PR China
[b] Laboratory for Marine Geology, Qingdao National Laboratory for Marine Science and Technology, 266061 Qingdao, PR China
[c] State Key Laboratory of Estuarine and Coastal Research, East China Normal University, 200062 Shanghai, PR China
[d] Centre for Past Climate Studies and Arctic Research Centre, Department of Geoscience, Aarhus University, DK-8000 Aarhus C, Denmark
[e] Department of Geology, Quaternary Sciences, Lund University, 22362 Lund, Sweden
[f] Alfred Wegener Institute Helmholtz Centre for Polar and Marine Research, D-28359 Bremerhaven, Germany
[g] Department of Physics and Astronomy, Aarhus University, DK-8000 Aarhus C, Denmark

ARTICLE INFO

Article history:
Received 17 April 2015
Received in revised form
30 October 2015
Accepted 2 November 2015
Available online 14 November 2015

Keywords:
Sea-ice variability
Solar activity
West Greenland
Last millennium

ABSTRACT

Arctic sea ice represents an important component of the climate system, and the present reduction of sea ice in the Arctic is of major concern. Despite its importance, little is known about past changes in sea-ice cover and the underlying forcing mechanisms. Here, we use diatom assemblages from a marine sediment core collected from the West Greenland shelf to reconstruct changes in sea-ice cover over the last millennium. The proxy-based reconstruction demonstrates a generally strong link between changes in sea-ice cover and solar variability during the last millennium. Weaker (or stronger) solar forcing may result in the increase (or decrease) in sea-ice cover west of Greenland. In addition, model simulations show that variations in solar activity not only affect local sea-ice formation, but also control the sea-ice transport from the Arctic Ocean through a sea-ice–ocean–atmosphere feedback mechanism. The role of solar forcing, however, appears to have been more ambiguous during an interval around AD 1500, after the transition from the Medieval Climate Anomaly to the Little Ice Age, likely to be driven by a range of factors.

1. Introduction

Sea ice is a key component of Earth's climate system, since it is an effective insulator between the oceans and the atmosphere, restricting the exchange of heat, mass, momentum and chemical constituents (Divine and Dick, 2006). In addition, it is essential for the powerful 'ice-albedo' feedback mechanism that amplifies climate variability at high latitudes (Forster et al., 2007). The ongoing severe reduction of Arctic sea ice is largely ascribed to anthropogenic effects, but the current rate of sea-ice reduction is much faster than predicted by models, with rates exceeding the expected effect from temperature change (IPCC, 2013). The factors controlling sea-ice variability are poorly understood, and the provision of sea-ice reconstructions extending back in time beyond the instrumental and satellite era is therefore critical (Massé et al., 2008; Müller et al., 2009; Stein et al., 2012; Belt and Müller, 2013; Collins et al., 2013; de Vernal et al., 2013; Weckström et al., 2013).

One factor, hitherto not thoroughly tested, is the role of the Sun in influencing the distribution of sea ice. Several studies indicate that multidecadal- to centennial-scale climate change during the last millennium was dominated by solar variability (Shindell et al., 1999; Rind, 2002; Gray et al., 2010). Solar activity has been shown to influence key components of the climate system, such as temperature, winds, precipitation, ocean circulation and iceberg transport (e.g. Verschuren et al., 2000; Bond et al., 2001; Hodell et al., 2001; Andrews et al., 2003; Jiang et al., 2005; Sejrup et al., 2010; Martin-Puertas et al., 2012; Knudsen et al., 2014; Moffa-Sánchez et al., 2014a; Jiang et al., 2015). However, only a few studies

* Corresponding author. Key Laboratory of Geographic Information Science, East China Normal University, 200062 Shanghai, PR China.
E-mail address: shalongbin@hotmail.com (L. Sha).

http://dx.doi.org/10.1016/j.quascirev.2015.11.002
0277-3791/

have investigated the link between variations in sea-ice proxies from the North Atlantic and solar variability on multidecadal to centennial time scales (e.g. Müller et al., 2012; Sha et al., 2014).

The central West Greenland shelf region is characterised by extensive sea-ice cover in the north and by almost sea-ice free waters in the south (Fig. 1) and is thus an ideal region for the study of short- and long-term sea-ice variability. The north-flowing West Greenland Current (WGC), which dominates the surface waters of the area, consists of two components. The upper part is dominated by Polar Water (T < 1 °C; S < 34 PSU) derived from the East Greenland Current (EGC) carrying a steady stream of multi-year ice along the East Greenland coast throughout the year, while the lower part of the WGC primarily consists of Atlantic-sourced water originating from the Irminger Current (IC) (T~4.5 °C; S > 34.95 PSU) (Buch, 2002) (Fig. 1). During winter and spring, the Baffin Current conveys large amounts of sea ice from Baffin Bay to Davis Strait and the Labrador Sea. At this time of year, sea ice normally covers most of Davis Strait north of 65°N. South of 65–67°N, the eastern Labrador Sea is mostly ice free, although sea ice may occur briefly during spring or late winter, as well as during early summer, if multi-year ice, originating from the Arctic Ocean, drifts into the area (Hansen et al., 2004).

Diatoms are marine siliceous algae which have been used successfully for reconstructing past sea-ice conditions (Crosta et al., 1998; Gersonde and Zielinski, 2000; Justwan and Koç Karpuz, 2008; Allen et al., 2011; Collins et al., 2012; Sha et al., 2014). It has further been demonstrated that diatom records from the study region can be used for quantitative reconstruction of April sea-ice variability (see Materials and methods and Supplementary material) (Sha et al., 2014). Here, we reconstruct changes in April sea-ice concentration (SIC) over the last millennium based on high-resolution diatom data from marine sediment core GA306-GC4 (see Materials and methods) (Sha et al., 2012), located off West Greenland, in order to study the sea-ice variability of the last millennium and to test for possible links to solar forcing. The site is located in the boundary zone between a northerly area dominated by sea ice in spring and a southerly area with a predominant absence of spring sea-ice cover (Fig. 1).

2. Materials and methods

2.1. Coring

Gravity core GA306-GC4 (66°44′41″N, 53°56′25″W; 502-cm long) and box core GA306-BC4 (35-cm long) were retrieved from the same location in a water depth of 445 m, in the Holsteinsborg Dyb basin off Kangerlussuaq, West Greenland, during the *Galathea 3 Expedition*, Leg 3, 25 August to 8 September 2006 (Fig. 1). Diatom samples were extracted from 1-cm thick slices taken at 5-cm intervals from core GA306-GC4, yielding a mean time resolution of ca. 10 years. The results of the diatom analyses from GA306-BC4 have previously been presented by Sha et al. (2014) and are given in the Supplementary material (Fig. S4), and the diatom assemblage data from GA306-GC4 have been published by Sha et al. (2012).

2.2. Chronology

The age–depth model for gravity core GA306-GC4 was constructed on the basis of a total of 11 ^{14}C ages of marine mollusc shells (10 from GA306-GC4 and one from GA306-BC4; see Table S1) (Erbs-Hansen et al., 2013). The samples were measured for radiocarbon content at the AMS ^{14}C Dating Centre, Aarhus University, Denmark. All of the ^{14}C dates were calibrated using the Marine09 calibration dataset (Reimer et al., 2009) with a ΔR of 140 ± 30 years (Erbs-Hansen et al., 2013), and the ^{14}C-based chronologies were constructed using the depositional model in the OxCal 4.1 software

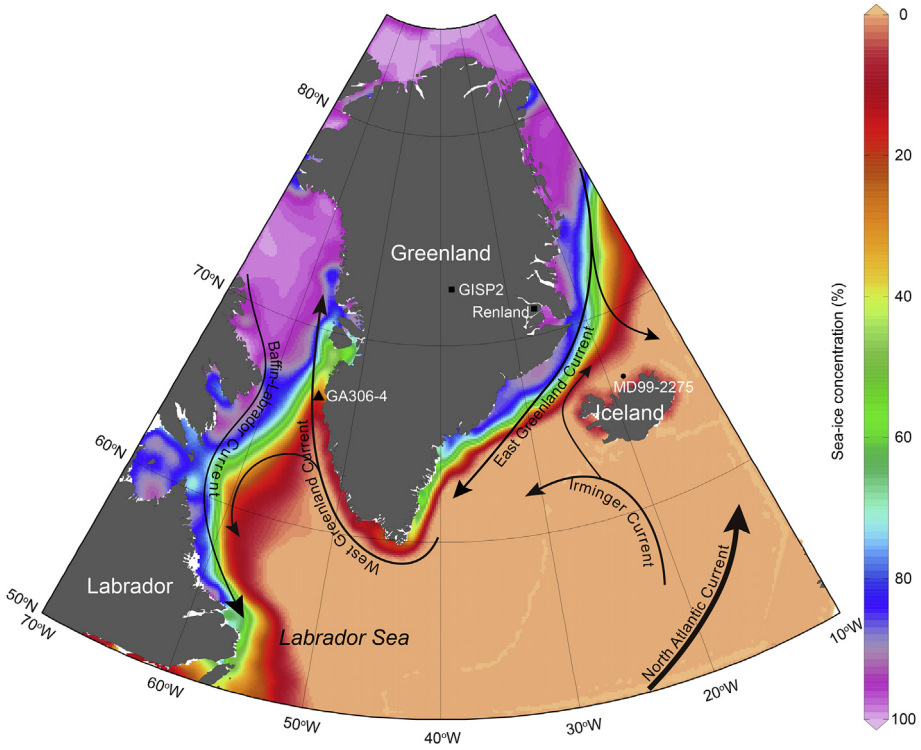

Fig. 1. Location of marine sediment cores GA306-4 (GA306-GC4 and GA306-BC4), and the other records referenced in the text, together with the modern surface circulation of the North Atlantic. The satellite April sea-ice concentration from Nimbus-7 SMMR and DMSP SSM/I-SSMIS Passive Microwave Data (GSFC product, NSIDC-0051) for the period AD 1979–2010 is also indicated.

(Ramsey, 2009) (see Fig. 2). It should be noted that a ΔR value of zero years was applied by Sha et al. (2012) for previously-published diatom data from core GA306-GC4, thus resulting in a slightly different age model than in the present paper. The depositional model was constructed using a *k* value of 150 (Fig. 2). The detailed age model of box core GA306-BC4 is based on ^{210}Pb dating (see Supplementary material and Sha et al., 2012).

2.3. Diatom-based transfer function for sea-ice concentration

A diatom sea-ice dataset, including the monthly mean of the SIC percentage (since 1979) is available from off West Greenland and around Iceland (Table S2). The results of canonical correspondence analysis (CCA) reveal that the diatom species predominantly influenced by the SIC generally have high values on the SIC 'axes', e.g. *Fragilariopsis cylindrus*, *Fossula arctica*, *Detonula confervaceae* resting spores and *Thalassiosira bulbosa*, and April SIC is the most important environmental factor controlling the distribution of diatoms (see Fig. S2 and Sha et al., 2014). Therefore, April SIC is an important climatic variable that may potentially be reconstructed back in time beyond the period of instrumental data (for detailed information see Supplementary material and Sha et al., 2014).

Seven numerical reconstruction methods were tested, and a weighted averaging with partial least squares regression (WA-PLS) using 3 components, which has the lowest root-mean squared error of prediction based on the leave-one-out jack-knifing $RMSEP_{(Jack)}$ (1.065) and the highest coefficient of determination between observed and predicted values R^2_{Jack} (0.916), was used quantitatively to reconstruct past SICs from the diatom assemblages, based on a modern database (Table S3). Comparison of observed values with predicted values (using a cross-validated model) based on diatom data from the same surface samples reveals a good linear relationship (see Supplementary material and Fig. S3).

The reliability of the diatom-based SIC reconstruction was further tested by comparing the reconstructed SIC record of the last ~75 years from box core GA306-BC4 at the same location as the studied core GA306-GC4, with the satellite SIC data for 1979–2006, and with the model SIC data from the HadISST 1.1 dataset during 1953–2006 (Rayner et al., 2003) (for detailed information see Supplementary material and Sha et al., 2014).

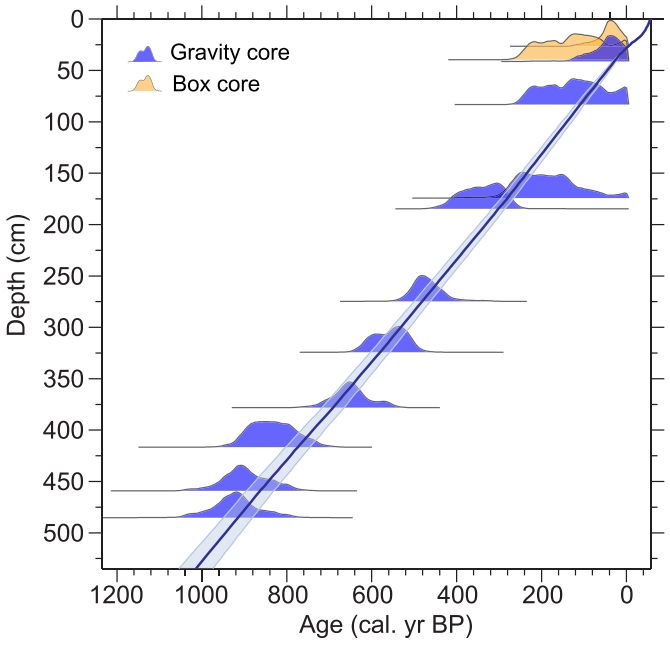

Fig. 2. Age–depth model for gravity core GA306-GC4.

2.4. Statistical significance

Running correlation coefficients of the SIC versus ^{14}C production rate were calculated for data in 250-year sliding windows, which includes a random phase test that takes into account the autocorrelations present in the time series (Ebisuzaki, 1997). The statistical significance of the correlation between changes in the SIC and ^{14}C production rate was evaluated based on comparisons to synthetic red-noise time series data. The synthetic data were modelled as a first-order autoregressive (AR1) process, following the procedure of Schulz and Mudelsee (2002), with a characteristic memory factor (ϕ) equal to that obtained for the raw SIC data. A total of 10,000 synthetic SIC datasets were simulated using a Monte Carlo approach, and the correlation coefficients obtained between the synthetic SIC data and ^{14}C production rate were compared to those obtained for the actual SIC data. This makes it possible to estimate the probability (p) of obtaining high correlations by chance.

2.5. Spectral and wavelet analyses

The power spectrum of the reconstructed SIC record was computed using the public domain software program REDFIT, which applies the Lomb-Scargle Fourier transform (Schulz and Mudelsee, 2002). Similar to the more traditional Fourier analysis, the Lomb-Scargle method is based on a least-squares fit of sinusoids to the time series data. The univariate spectra were bias-corrected using 1000 Monte-Carlo simulations. REDFIT automatically produces first-order autoregressive (AR1) time series with sampling times and characteristic time scales matching those of the real climate data. To assess the statistical significance of a spectral peak, REDFIT estimates the upper confidence interval of the AR1 noise for various significance levels based on a χ^2 distribution.

Wavelet analysis was carried out in MATLAB using the wavelet coherence (WTC) software package of Grinsted et al. (2004). Prior to the wavelet analysis, the data were normalized by subtracting the mean value and dividing by the standard deviation. The unevenly spaced data were linearly interpolated to an evenly spaced time scale. The time series were padded with zeros to dampen edge effects and reduce spectral leakage, which results in underestimation of the lowest frequencies near the edges. The cone of influence defines the region that is likely to be influenced by this effect. The relative lag between time series was inspected using the phase arrows.

2.6. Model description and experimental design

The comprehensive climate model COSMOS (ECHAM5-JSBACH-MPIOM) was used to evaluate the role played by changes in solar radiation on sea-ice cover at the core sites. The model configuration included the atmosphere component ECHAM5 (Roeckner et al., 2003) at T31 resolution (~3.75°) with 19 vertical layers, complemented by a land-surface scheme including dynamical vegetation (JSBACH) (Brovkin et al., 2009). The ocean component MPI-OM (Marsland et al., 2003), including the dynamics of sea ice formulated using viscous-plastic rheology (Hibler, 1979), has an average horizontal resolution of 3° × 1.8° with 40 uneven vertical layers. The climate model was previously utilized to analyse the climate of the last millennium (Jungclaus et al., 2010), the last glacial (Zhang et al., 2013, 2014) and the last interglacial period (Varma et al., 2012; Wei and Lohmann, 2012; Wei et al., 2012), as well as warm climates of the Miocene (Knorr et al., 2011; Knorr and Lohmann, 2014) and the Pliocene (Stepanek and Lohmann, 2012; Dowsett et al., 2013).

To evaluate the corresponding changes in SIC, two sensitivity experiments with high and low solar radiation anomalies (1367 ± 3 W/m^2) were performed under pre-industrial (PI) conditions. Both simulations were initialized from the PI ocean condition and integrated for 100 model years to quasi-equilibrium. The last 30 model years were assumed to represent the corresponding climatology.

3. Changes in sea-ice concentration and their regional significance

The reconstructed SICs at Holsteinsborg Dyb off West Greenland varied between 30 and 60% over the last millennium (Fig. 3e). The SICs were generally low during the interval AD 900–1400, albeit with relatively higher values around AD 1050. This suggests that, apart from a short period of enhanced sea-ice cover, low SIC generally prevailed during the Medieval Climate Anomaly (MCA). A distinct shift to generally higher SICs occurred around AD 1400 and lasted until AD 1900, at which point the SIC started to decline. The Little Ice Age (LIA) was thus characterised by severe sea-ice conditions at Holsteinsborg Dyb, as indicated by maximum SIC values around AD 1450–1500, AD 1650–1700 and AD 1800.

A similar increase in sea-ice cover during the LIA has been recognized in a number of records from along the West Greenland coast (Lassen et al., 2004; Roncaglia and Kuijpers, 2004; Lloyd, 2006; Seidenkrantz et al., 2007), although some records suggest an earlier (Seidenkrantz et al., 2008) or later (Ribeiro et al., 2012) onset of strong sea-ice conditions in the Disko Bugt area. Reconstruction of the mid-Holocene SIC record for the Vaigat Strait based on the same diatom SIC transfer function indicates that an extensive sea-ice cover occurred after ca. AD 1300, coinciding with the LIA (Sha et al., 2014). In the eastern and western Fram Strait, significantly higher IRD (ice rafted debris) and IP$_{25}$ contents were attributed to heavy sea-ice conditions during the LIA (Werner et al., 2011; Müller et al., 2012), and Bonnet et al. (2010) found a major transition to increased sea-ice cover during the later phase of the LIA on the West Spitsbergen margin. Similar cold conditions, as well as persistent sea-ice cover, were also described in sea-surface temperature reconstructions derived from diatoms and alkenones on the North Icelandic shelf (Jiang et al., 2005; Sicre et al., 2008), implying the strong influence of Polar waters from the EGC during the LIA.

Further afield, the concentration of sea-salt ion (Na$^+$) in the Greenland Ice Sheet Project 2 (GISP2) ice core (Mayewski et al., 1997) (Fig. 3d), which may be linked to sea surface windiness and/or sea-ice openness (Kreutz et al., 1997; Mayewski et al., 2002), indicates a shift to higher values around AD 1400. A generally similar pattern was also shown by the organic geochemistry sea-ice

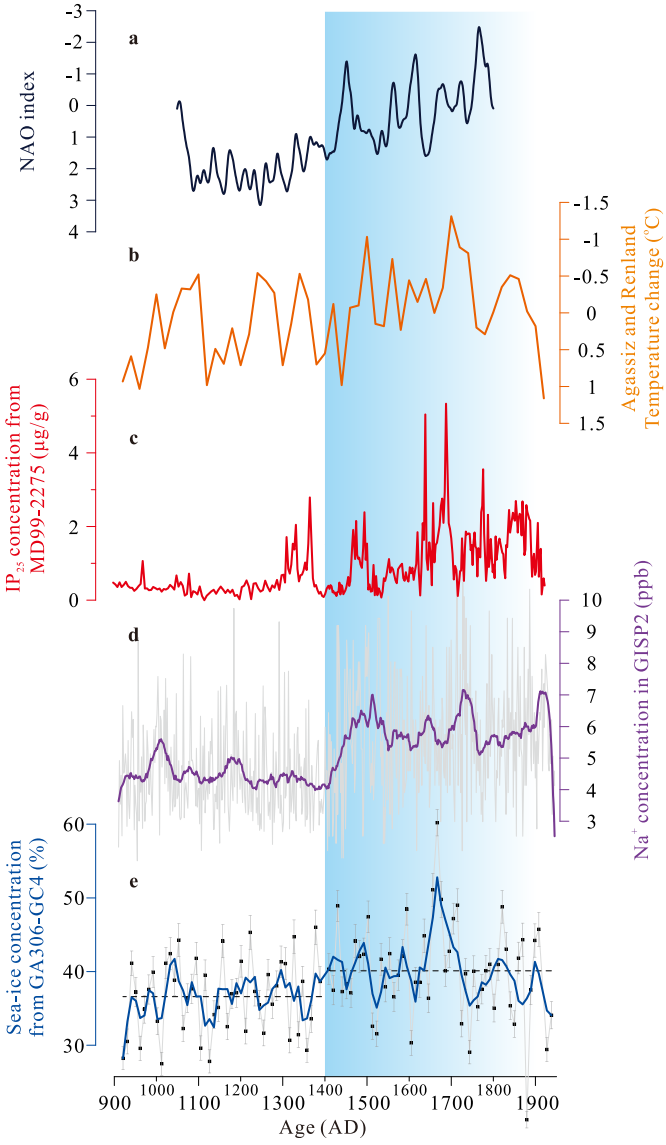

Fig. 3. (a) Reconstructed NAO index (dark blue curve) (Trouet et al., 2009). (b) Temperature reconstruction from the Agassiz and Renland ice cores (orange curve) (Vinther et al., 2009). (c) The organic geochemistry sea-ice proxy IP$_{25}$ record from core MD99-2275 (red curve) (Massé et al., 2008). (d) Sea-salt ion (Na$^+$) concentration in the GISP2 ice core (purple curve) (Mayewski et al., 1997). (e) Diatom-based sea-ice concentration reconstruction from core GA306-GC4 (blue curve). Actual data are shown as grey lines; smoothed records (20-year running averages) are denoted by bold lines in colour. The dashed grey lines in Fig. 3e indicate the average values before and after AD 1400.

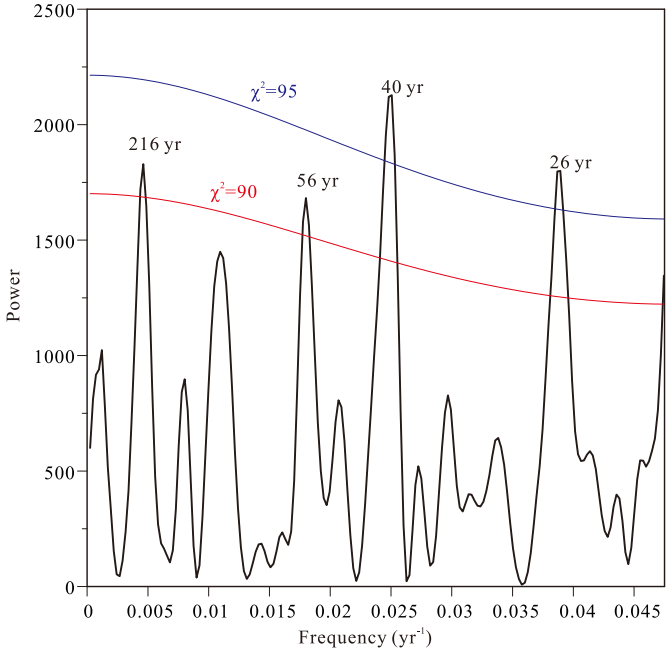

Fig. 4. Spectral analysis (Lomb-Scargle Fourier transform) of the reconstructed sea-ice concentration from gravity core GA306-GC4. The coloured lines indicate the 95% (blue) and 90% (red) red-noise false-alarm levels calculated using REDFIT. (For interpretation of the references to colour in this figure legend, the reader is referred to the web version of this article.)

proxy IP_{25} from MD99-2275 (Massé et al., 2008) (Fig. 3c), which records fluctuations in the presence of sea ice north of Iceland. After AD 1400, both the IP_{25} abundance and the sea-salt ions exhibit much higher values than for the earlier period, in particular around AD 1500 and AD 1700, indicating colder conditions, as well as persistent sea-ice cover during the LIA. Furthermore, both proxy records indicate a decline in SIC that started around AD 1900. Our SIC reconstruction is also in broad agreement with the temperature record from the Agassiz and Renland ice cores (Vinther et al., 2009) (Fig. 3b), which exhibits warm conditions before about AD 1400, and a marked temperature shift from the MCA to the so-called LIA.

In addition, there is a high degree of consistency between our sea-ice record and the proxy-based reconstruction of the North Atlantic Oscillation (NAO) index of Trouet et al. (2009) (Fig. 3a). NAO is today defined as the sea-level pressure difference between the Icelandic Low and the Azores High pressure system (Hurrell, 1995). A shift to a prevalent negative NAO index at the MCA-LIA transition, which may be consistent with enhanced storm intensity rather than storm frequency (Trouet et al., 2012; Moffa-Sánchez et al., 2014b), implies overall weakened westerlies in the North Atlantic during the LIA when total solar irradiance was low. The weaker westerlies would reduce heat loss over the Labrador Sea (Moffa-Sánchez et al., 2014b) and poleward transport of Atlantic waters (Sejrup et al., 2010), thereby enhancing the southward export of Polar waters and Arctic sea ice through Fram Strait (Müller et al., 2012; Moffa-Sánchez et al., 2014b) facilitating an increased sea-ice transport by the EGC and WGC (cf. Kuijpers et al., 2014).

The similarity between the sea-ice conditions off West Greenland and north of Iceland and the ice-core temperature record suggests that the environmental changes revealed in our record are regionally significant.

Historical archives show that the Norse colonization of Greenland began around AD 895 and terminated around AD 1400 (Buckland et al., 1996). A shift towards severe sea-ice conditions after ca. AD 1400 supports the argument that expansion of sea ice at the beginning of the LIA played a critical role in the demise of Norse settlements in Greenland (Kuijpers et al., 2014).

The power spectrum of the SIC record for the last millennium exhibits statistically significant periodicities ($p < 0.05$) centred around 40 and 26 years, as well as ~216 and 56 years ($p < 0.10$) (Fig. 4), suggesting oscillatory climatic changes at multidecadal to centennial time scales.

4. Discussion

The SIC record roughly co-varies with minima in solar activity, particularly during the Oort Minimum (AD 1040–1080), the Maunder Minimum (AD 1645–1715) and the Dalton Minimum (AD 1790–1820) (Schröder, 2005) (Fig. 5). This suggests the possible impact of solar activity on sea-ice variability during the last millennium.

In order to test the role of solar activity on sea-ice variability, we evaluated the relationship between our SIC reconstruction record from the West Greenland shelf and variations in the ^{14}C production rate (Fig. 5a), a proxy for past solar variability inferred from atmospheric ^{14}C concentrations measured in tree rings (Muscheler et al., 2007; Reimer et al., 2009). The running correlation coefficients indicate a robust positive correlation between SIC and the ^{14}C production rate at statistically significant levels ($p < 0.1$) for the last millennium, except during the Spörer Minimum (AD 1460–1550) (Fig. 5b and c). It should be noted, however, that the absence of a statistically significant solar influence on sea-ice variability around AD 1500 may reflect the complexity of the

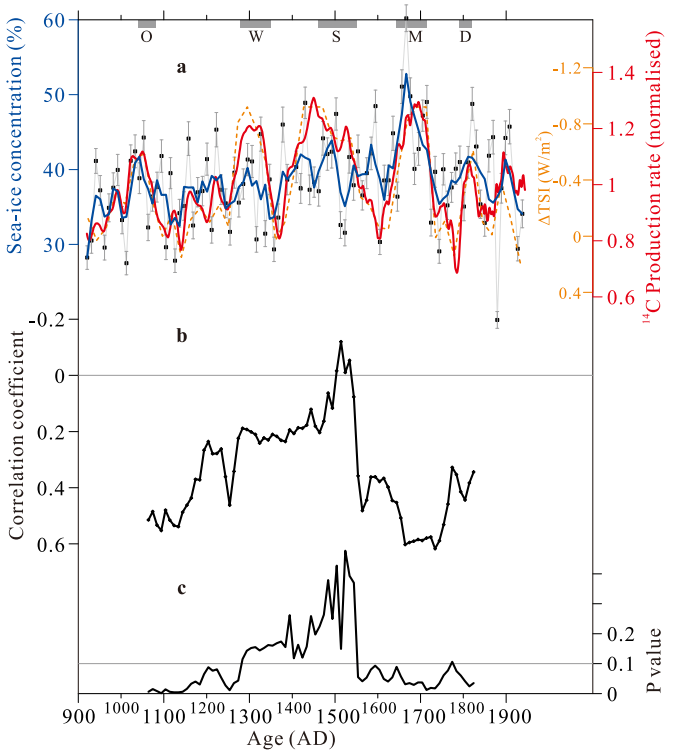

Fig. 5. Reconstructed sea-ice concentrations from core GA306-GC4 compared to the ^{14}C production rate corrected for the fossil fuel (Suess) effect for the period from 1850 to 1950 AD (Muscheler et al., 2007). (a) The direct comparison of sea-ice concentration (blue) and ^{14}C production rate (red), as well as with ΔTSI (orange; difference of total solar irradiance from 1365.57 W/m^2) (Steinhilber et al., 2012). (b) The running correlation coefficient between sea-ice concentration and ^{14}C data (calculated for moving 250 year windows). (c) The results of a significance analysis indicating highly significant positive correlations for the early and latter part of the last millennium. The well-documented periods of solar minima are indicated by the shaded areas at the top of the figure.

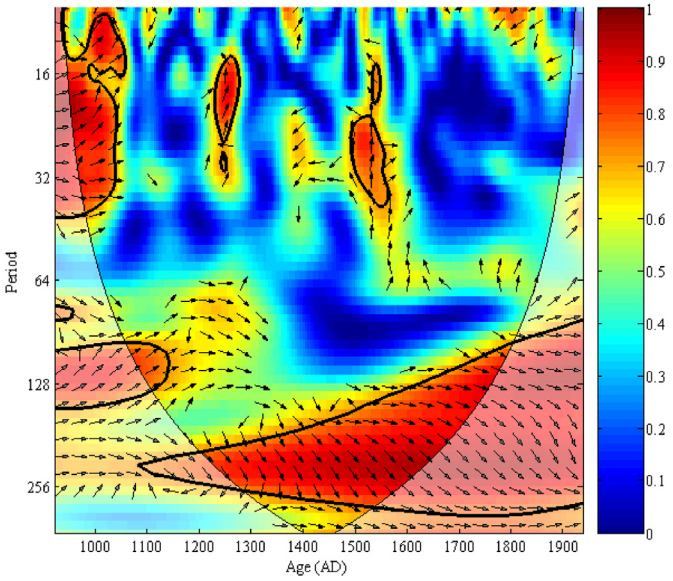

Fig. 6. Wavelet coherence analysis of sea-ice concentration and ^{14}C production rate (Grinsted et al., 2004). Both records are interpolated onto a regular time grid with a constant spacing of 5 years. The black boundary indicates the 95% significance level. The vectors indicate the relative phase relationship: arrows pointing to the right indicate common in-phase variations in both records.

climate system during the transition from the MCA to the LIA. This MCA-LIA climate transition, consistent with a suggested shift to more negative NAO conditions (Seidenkrantz et al., 2007, 2008; Trouet et al., 2009, 2012; Olsen et al., 2012; Sicre et al., 2014), may be attributed to some combination of explosive volcanism (Miller et al., 2012) and reductions in solar irradiance, especially the Spörer Minimum. A cross-correlation analysis further shows that the maximum correlation is obtained at zero lag (Fig. S6).

In addition, the significant 216-year period is similar to the well-known de Vries solar cycle of ~210 years, while the periodicity of 26 years may be related to the periodicity of the 22-year Hale cycle (Fig. 4). We note, however, that the latter periodicity (~26 years) lies close to the Nyquist period and therefore may be an artefact of the sampling frequency. Notably, the 56-year cycle in our sea-ice record is not associated with any well-known solar cycles, but falls within the range of the 55–70 year spectrum calculated for the Atlantic Multidecadal Oscillation (AMO) over the last 8000 years (Knudsen et al., 2011), although the sea-ice variability linked to solar forcing may also have impacted the AMO cycle (Knudsen et al., 2014).

Wavelet coherence analyses further indicate a significant degree of coherency between the reconstructed SIC and the ^{14}C production rate over the last millennium, in particular for periods in the range

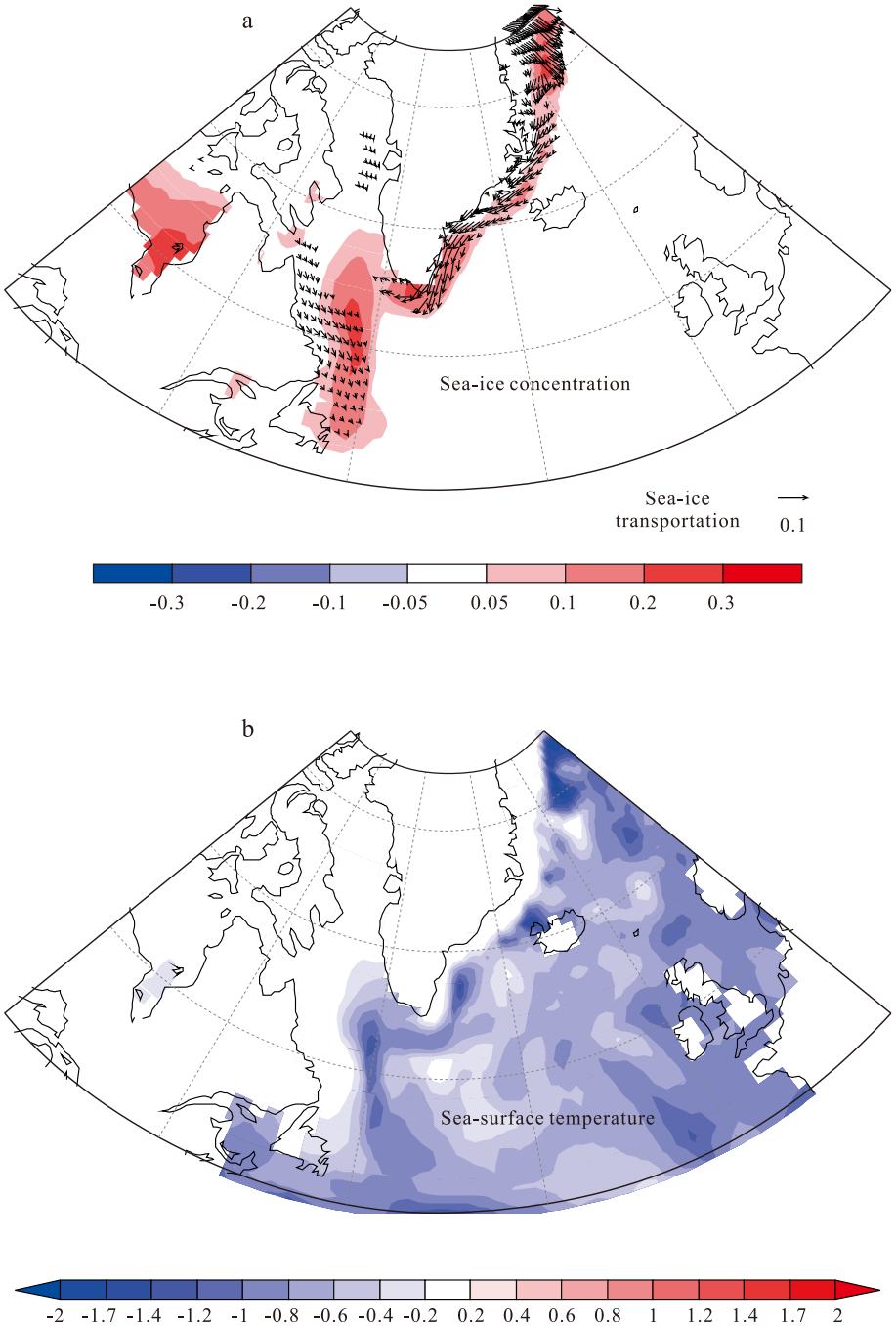

Fig. 7. (a) Anomalous fields of simulated sea-ice concentration (shaded, %) and sea-ice transportation (vector, m^2/s) between negative and positive solar radiation experiments. (b) Simulated sea-surface temperature anomaly (shaded, °C) between negative and positive solar radiation experiments.

180–260 years (Fig. 6). It is, therefore, likely that solar variability has influenced sea-ice cover off West Greenland on multidecadal to centennial time scales.

To investigate the feedback processes linking solar activity and sea-ice cover, we used the coupled climate model COSMOS, which indicates that a decrease in solar radiation results in increased sea-ice cover (Fig. 7a) and decreased sea-surface temperature (Fig. 7b). A strong negative correlation between sea-ice variability and solar forcing is observed along the eastern and southwestern coast of Greenland and in the Arctic Ocean, indicating that in this model solar variability is critical for simulating changes in local sea-ice production. A small change in incoming shortwave radiation, and associated ice-albedo effects, resulted in a large response of local ice formation, according to 'bottom-up' (solar heating of the sea surface) mechanisms (Gray et al., 2010; Hunke et al., 2010).

Our modelling results further suggest that increased sea-ice production in the Arctic Ocean due to weaker solar forcing would result in an increased southward transport of sea ice from the Arctic Ocean and subsequently to an increased transport of sea ice into the eastern Labrador Sea by the EGC (Fig. 7a). This result is in accordance with modern oceanographic observations from off the coast of West Greenland, which indicate that variations in sea-ice cover are caused by changes not only in local ice production (first-year ice), but also in the transport of specifically multi-year ice from the Arctic Ocean by the EGC, continuing northwards off West Greenland assisted by the WGC (Schmith and Hansen, 2003) (Fig. 1). An increased southward transport of Arctic sea ice via the EGC during the LIA is also evidenced by the IP_{25} sea-ice proxy record from north of Iceland (Massé et al., 2008) (Fig. 3c) and the Fram Strait (Müller et al., 2012).

The proxy evidence and modelling results presented here support the link between sea-ice cover off West Greenland and solar variability, as well as with the large-scale (surface) ocean circulation, indirectly inferred from the modelled sea-ice transportation. Weaker (or stronger) solar forcing may result in the increase (or decrease) in SICs west of Greenland and the extreme sensitivity of sea ice to climatic changes would further amplify variations in the SICs.

The export of sea ice and freshwater from the Arctic Ocean into the North Atlantic may impact the rate of deep-water formation and the thermohaline circulation (Mauritzen and Häkkinen, 1997; Holland et al., 2001; Rigor et al., 2002). During periods of low solar activity, cooler and less saline water from the North Atlantic is advected into the Arctic Ocean, leading to an increase in freshwater and sea-ice cover in the Arctic Ocean (Ruzmaikin et al., 2004). Sea ice export from the Arctic provides significant freshwater forcing for the sensitive regions of deep-water formation (Holland et al., 2001), and increased export of freshwater leads to the diminished production of intermediate and deep water masses through ocean convection (Schmith and Hansen, 2003). Consequently, the subpolar gyre and the Atlantic Meridional Overturning Circulation (AMOC) are weakened (Mauritzen and Häkkinen, 1997), which in turn reduces the transport of heat into the Arctic Ocean, causing further sea-ice growth (Sedláček and Mysak, 2009; Lehner et al., 2013). Furthermore, as deep convection weakens, it reduces the import of heat, reinforcing the expansion of the sea ice (Lehner et al., 2013).

The present study demonstrates that changes in solar activity would have the potential to initiate a self-amplifying sea-ice response during the last millennium, which in turn would affect the thermohaline circulation. This strongly highlights the fact that the current climatic warming is disrupting a very complex and sensitive system, with potentially unforeseen consequences for future sea-ice cover.

Acknowledgements

The core material was obtained from the *Galathea 3 Expedition* cruise in 2006. We are grateful to the captain, crew and expedition members for coring and seismic operations on board HMS *Vædderen* and all cruises providing surface samples for our study. We thank Jan Heinemeier, Aarhus University, Denmark, for providing the ^{14}C age determinations and Thorbjørn Joest Andersen, University of Copenhagen, Denmark, for the ^{210}Pb datings. Financial support for this work was provided by the Natural Science Foundation of China (Grants 41176048, 41406209) and the Chinese Polar Environment Comprehensive Investigation & Assessment Programmes (Grant CHINARE2014-03-02), as well as the European Union's Sevenths Framework Programme (FP7/2007e2013) "Past4Future" Climate Change – Learning from the Past Climate (Grant 243908), and the Danish Council for Independent Research, Natural Science (projects 09-071321 and 12-126709). RM was supported by a grant from the Swedish Research Council (Dnr: 2013-8421). This work is also a contribution to the PAGES sea-ice proxy (SIP) working group and the Taishan Scholars Program of Shandong. Finally, we are grateful to Dr. Juliane Müller and two anonymous referees for valuable comments and to Dr. Jan Bloemendal for correction of the English text.

Appendix A. Supplementary data

Supplementary data related to this article can be found at http://dx.doi.org/10.1016/j.quascirev.2015.11.002.

References

Allen, C.S., Pike, J., Pudsey, C.J., 2011. Last glacial–interglacial sea-ice cover in the SW Atlantic and its potential role in global deglaciation. Quat. Sci. Rev. 30, 2446–2458.
Andrews, J.T., Hardadottir, J., Stoner, J.S., Mann, M.E., Kristjansdottir, G.B., Koç Karpuz, N., 2003. Decadal to millennial-scale periodicities in North Iceland shelf sediments over the last 12 000 cal yr: long-term North Atlantic oceanographic variability and solar forcing. Earth Planet. Sci. Lett. 210, 453–465.
Belt, S.T., Müller, J., 2013. The Arctic sea ice biomarker IP25: a review of current understanding, recommendations for future research and applications in palaeo sea ice reconstructions. Quat. Sci. Rev. 79, 9–25.
Bond, G., Kromer, B., Beer, J., Muscheler, R., Evans, M.N., Showers, W., Hoffmann, S., Lotti-Bond, R., Hajdas, I., Bonani, G., 2001. Persistent solar influence on North Atlantic climate during the Holocene. Science 294, 2130–2136.
Bonnet, S., de Vernal, A., Hillaire-Marcel, C., Radi, T., Husum, K., 2010. Variability of sea-surface temperature and sea-ice cover in the Fram Strait over the last two millennia. Mar. Micropaleontol. 74, 59–74.
Brovkin, V., Raddatz, T., Reick, C.H., Claussen, M., Gayler, V., 2009. Global biogeophysical interactions between forest and climate. Geophys. Res. Lett. 36, L07405.
Buch, E., 2002. Present Oceanographic Conditions in Greenland Waters, pp. 1–36. Danish Meteorological Institute Scientific Report, Copenhagen.
Buckland, P.C., Amorosi, T., Barlow, L.K., Dugmore, A.J., Mayewski, P.A., McGovern, T.H., Ogilvie, A.E.J., Sadler, J.P., Skidmore, P., 1996. Bioarchaeological and climatological evidence for the fate of Norse farmers in Medieval Greenland. Antiquity 70, 88–96.
Collins, L.G., Allen, C.S., Pike, J., Hodgson, D.A., Weckström, K., Massé, G., 2013. Evaluating highly branched isoprenoid (HBI) biomarkers as a novel Antarctic sea-ice proxy in deep ocean glacial age sediments. Quat. Sci. Rev. 79, 87–98.
Collins, L.G., Pike, J., Allen, C.S., Hodgson, D.A., 2012. High-resolution reconstruction of southwest Atlantic sea-ice and its role in the carbon cycle during marine isotope stages 3 and 2. Paleoceanography 27, PA3217.
Crosta, X., Pichon, J.J., Burckle, L.H., 1998. Application of modern analog technique to marine Antarctic diatoms: reconstruction of maximum sea-ice extent at the Last Glacial Maximum. Paleoceanography 13, 284–297.
de Vernal, A., Gersonde, R., Goosse, H., Seidenkrantz, M.-S., Wolff, E.W., 2013. Sea ice in the paleoclimate system: the challenge of reconstructing sea ice from proxies – an introduction. Quat. Sci. Rev. 79, 1–8.
Divine, D.V., Dick, C., 2006. Historical variability of sea ice edge position in the Nordic Seas. J. Geophys. Res. 111, C01001.
Dowsett, H.J., Foley, K.M., Stoll, D.K., Chandler, M.A., Sohl, L.E., Bentsen, M., Otto-Bliesner, B.L., Bragg, F.J., Chan, W.-L., Contoux, C., Dolan, A.M., Haywood, A.M., Jonas, J.A., Jost, A., Kamae, Y., Lohmann, G., Lunt, D.J., Nisancioglu, K.H., Abe-Ouchi, A., Ramstein, G., Riesselman, C.R., Robinson, M.M., Rosenbloom, N.A., Salzmann, U., Stepanek, C., Strother, S.L., Ueda, H., Yan, Q., Zhang, Z., 2013. Sea

surface temperature of the mid-Piacenzian ocean: a data-model comparison. Sci. Rep. 3.
Ebisuzaki, W., 1997. A method to estimate the statistical significance of a correlation when the data are serially correlated. J. Clim. 10, 2147–2153.
Erbs-Hansen, D.R., Knudsen, K.L., Olsen, J., Lykke-Andersen, H., Underbjerg, J.A., Sha, L., 2013. Paleoceanographical development off Sisimiut, West Greenland, during the mid- and late Holocene: a multiproxy study. Mar. Micropaleontol. 102, 79–97.
Forster, P., Ramaswamy, V., Artaxo, P., Berntsen, T., Betts, R., Fahey, D.W., Haywood, J., Lean, J., Lowe, D.C., Myhre, G., Nganga, J., Prinn, R., Raga, G., Schulz, M., Van Dorland, R., 2007. Changes in atmospheric constituents and in radiative forcing. In: Solomon, S., Qin, D., Manning, M., Chen, Z., Marquis, M., Averyt, K.B., Tignor, M., Miller, H.L. (Eds.), Climate Change 2007: the Physical Science Basis. Contribution of Working Group I to the Fourth Assessment Report of the Intergovernmental Panel on Climate Change. Cambridge University Press, Cambridge, United Kingdom and New York, NY, USA.
Gersonde, R., Zielinski, U., 2000. The reconstruction of late Quaternary Antarctic sea-ice distribution—the use of diatoms as a proxy for sea-ice. Palaeogeogr. Palaeoclimatol. Palaeoecol. 162, 263–286.
Gray, L.J., Beer, J., Geller, M., Haigh, J.D., Lockwood, M., Matthes, K., Cubasch, U., Fleitmann, D., Harrison, G., Hood, L., Luterbacher, J., Meehl, G.A., Shindell, D., van Geel, B., White, W., 2010. Solar influence on climate. Rev. Geophys. 48, RG4001.
Grinsted, A., Moore, J.C., Jevrejeva, S., 2004. Application of the cross wavelet transform and wavelet coherence to geophysical time series. Nonlinear Process. Geophys. 11, 561–566.
Hansen, K.Q., Buch, E., Gregersen, U., 2004. Weather, Sea and Ice Conditions Offshore West Greenland – Focusing on New License Areas 2004, pp. 1–31. Danish Meteorological Institute Scientific Report, Copenhagen.
Hibler, W.D., 1979. A dynamic thermodynamic sea ice model. J. Phys. Oceanogr. 9, 815–846.
Hodell, D.A., Brenner, M., Curtis, J.H., Guilderson, T., 2001. Solar forcing of drought frequency in the Maya Lowlands. Science 292, 1367–1370.
Holland, M.M., Bitz, C.M., Eby, M., Weaver, A.J., 2001. The role of ice–ocean interactions in the variability of the North Atlantic thermohaline circulation. J. Clim. 14, 656–675.
Hunke, E.C., Lipscomb, W.H., Turner, A.K., 2010. Sea-ice models for climate study: retrospective and new directions. J. Glaciol. 56, 1162–1172.
Hurrell, J.W., 1995. Decadal trends in the North Atlantic oscillation: regional temperatures and precipitation. Science 269, 676–679.
IPCC, 2013. In: Stocker, T.F., Qin, D., Plattner, G.-k., Tignor, M.M.B., Allen, S.K., Boschung, J., Nauels, A., Xia, Y., Bex, V., Midgley, P.M. (Eds.), Climate Change 2013: the Physical Science Basis. Contribution of Working Group I to the Fifth Assessment Report of the Intergovernmental Panel on Climate Change. Cambridge University Press, Cambridge, United Kingdom and New York, NY, USA, p. 1535.
Jiang, H., Eiríksson, J., Schulz, M., Knudsen, K.L., Seidenkrantz, M.-S., 2005. Evidence for solar forcing of sea-surface temperature on the North Icelandic Shelf during the late Holocene. Geology 33, 73–76.
Jiang, H., Muscheler, R., Björck, S., Seidenkrantz, M.-S., Olsen, J., Sha, L., Sjolte, J., Eiríksson, J., Ran, L., Knudsen, K.-L., Knudsen, M.F., 2015. Solar forcing of Holocene summer sea-surface temperatures in the northern North Atlantic. Geology 43, 203–206.
Jungclaus, J.H., Lorenz, S.J., Timmreck, C., Reick, C.H., Brovkin, V., Six, K., Segschneider, J., Giorgetta, M.A., Crowley, T.J., Pongratz, J., Krivova, N.A., Vieira, L.E., Solanki, S.K., Klocke, D., Botzet, M., Esch, M., Gayler, V., Haak, H., Raddatz, T.J., Roeckner, E., Schnur, R., Widmann, H., Claussen, M., Stevens, B., Marotzke, J., 2010. Climate and carbon-cycle variability over the last millennium. Clim. Past 6, 723–737.
Justwan, A., Koç Karpuz, N., 2008. A diatom based transfer function for reconstructing sea ice concentrations in the North Atlantic. Mar. Micropaleontol. 66, 264–278.
Knorr, G., Butzin, M., Micheels, A., Lohmann, G., 2011. A warm Miocene climate at low atmospheric CO_2 levels. Geophys. Res. Lett. 38, L20701.
Knorr, G., Lohmann, G., 2014. Climate warming during Antarctic ice sheet expansion at the Middle Miocene transition. Nat. Geosci. 7, 376–381.
Knudsen, M.F., Jacobsen, B.H., Seidenkrantz, M.-S., Olsen, J., 2014. Evidence for external forcing of the Atlantic Multidecadal Oscillation since termination of the Little Ice Age. Nat. Commun. 5, 3323.
Knudsen, M.F., Seidenkrantz, M.-S., Jacobsen, B.H., Kuijpers, A., 2011. Tracking the Atlantic Multidecadal Oscillation through the last 8,000 years. Nat. Commun. 2, 178.
Kreutz, K.J., Mayewski, P.A., Meeker, L.D., Twickler, M.S., Whitlow, S.I., Pittalwala, I.I., 1997. Bipolar changes in atmospheric circulation during the Little Ice Age. Science 277, 1294–1296.
Kuijpers, A., Mikkelsen, N., Ribeiro, S., Seidenkrantz, M.-S., 2014. Impact of Medieval Fjord hydrography and climate on the Western and Eastern settlements in Norse Greenland. J. N. Atl. 6, 1–13.
Lassen, S.J., Kuijpers, A., Kunzendorf, H., Hoffmann-Wieck, G., Mikkelsen, N., Konradi, P., 2004. Late-Holocene Atlantic bottom-water variability in Igaliku Fjord, South Greenland, reconstructed from foraminifera faunas. Holocene 14, 165–171.
Lehner, F., Born, A., Raible, C.C., Stocker, T.F., 2013. Amplified inception of European Little Ice Age by sea ice–ocean–atmosphere feedbacks. J. Clim. 26, 7586–7602.
Lloyd, J.M., 2006. Late Holocene environmental change in Disko Bugt, west Greenland: interaction between climate, ocean circulation and Jakobshavn Isbrae. Boreas 35, 35–49.
Müller, J., Masse, G., Stein, R., Belt, S.T., 2009. Variability of sea-ice conditions in the Fram Strait over the past 30,000 years. Nat. Geosci. 2, 772–776.
Müller, J., Werner, K., Stein, R., Fahl, K., Moros, M., Jansen, E., 2012. Holocene cooling culminates in sea ice oscillations in Fram Strait. Quat. Sci. Rev. 47, 1–14.
Marsland, S.J., Haak, H., Jungclaus, J.H., Latif, M., Röske, F., 2003. The Max-Planck-Institute global ocean/sea ice model with orthogonal curvilinear coordinates. Ocean Model. 5, 91–127.
Martin-Puertas, C., Matthes, K., Brauer, A., Muscheler, R., Hansen, F., Petrick, C., Aldahan, A., Possnert, G., van Geel, B., 2012. Regional atmospheric circulation shifts induced by a grand solar minimum. Nat. Geosci. 5, 397–401.
Massé, G., Rowland, S.J., Sicre, M.-A., Jacob, J., Jansen, E., Belt, S.T., 2008. Abrupt climate changes for Iceland during the last millennium: evidence from high resolution sea ice reconstructions. Earth Planet. Sci. Lett. 269, 565–569.
Mauritzen, C., Häkkinen, S., 1997. Influence of sea ice on the thermohaline circulation in the Arctic-North Atlantic Ocean. Geophys. Res. Lett. 24, 3257–3260.
Mayewski, P.A., Meeker, L.D., Twickler, M.S., Whitlow, S., Yang, Q., Lyons, W.B., Prentice, M., 1997. Major features and forcing of high-latitude northern hemisphere atmospheric circulation using a 110,000-year-long glaciochemical series. J. Geophys. Res. 102, 26345–26366.
Mayewski, P.A., White, F., Margulis, L., 2002. The Ice Chronicles: the Quest to Understand Global Climate Change. University of New Hampshire Press.
Miller, G.H., Geirsdóttir, Á., Zhong, Y., Larsen, D.J., Otto-Bliesner, B.L., Holland, M.M., Bailey, D.A., Refsnider, K.A., Lehman, S.J., Southon, J.R., Anderson, C., Björnsson, H., Thordarson, T., 2012. Abrupt onset of the Little Ice Age triggered by volcanism and sustained by sea-ice/ocean feedbacks. Geophys. Res. Lett. 39, L02708.
Moffa-Sánchez, P., Born, A., Hall, I.R., Thornalley, D.J.R., Barker, S., 2014a. Solar forcing of North Atlantic surface temperature and salinity over the past millennium. Nat. Geosci. 7, 275–278.
Moffa-Sánchez, P., Hall, I.R., Barker, S., Thornalley, D.J.R., Yashayaev, I., 2014b. Surface changes in the eastern Labrador Sea around the onset of the Little Ice Age. Paleoceanography 29, 2013PA002523.
Muscheler, R., Joos, F., Beer, J., Müller, S.A., Vonmoos, M., Snowball, I., 2007. Solar activity during the last 1000 yr inferred from radionuclide records. Quat. Sci. Rev. 26, 82–97.
Olsen, J., Anderson, N.J., Knudsen, M.F., 2012. Variability of the North Atlantic Oscillation over the past 5,200 years. Nat. Geosci. 5, 808–812.
Ramsey, C.B., 2009. Bayesian analysis of radiocarbon dates. Radiocarbon 51, 337–360.
Rayner, N.A., Parker, D.E., Horton, E.B., Folland, C.K., Alexander, L.V., Rowell, D.P., Kent, E.C., Kaplan, A., 2003. Global analyses of sea surface temperature, sea ice, and night marine air temperature since the late nineteenth century. J. Geophys. Res. 108, 4407.
Reimer, P.J., Baillie, M.G.L., Bard, E., Bayliss, A., Beck, J.W., Blackwell, P.G., Ramsey, C.B., Buck, C.E., Burr, G.S., Edwards, R.L., Friedrich, M., Grootes, P.M., Guilderson, T.P., Hajdas, I., Heaton, T.J., Hogg, A.G., Hughen, K.A., Kaiser, K.F., Kromer, B., McCormac, F.G., Manning, S.W., Reimer, R.W., Richards, D.A., Southon, J.R., Talamo, S., Turney, C.S.M., van der Plicht, J., Weyhenmeyer, C.E., 2009. IntCal09 and Marine09 radiocarbon age calibration curves, 0-50,000 years cal BP. Radiocarbon 51, 1111–1150.
Ribeiro, S., Moros, M., Ellegaard, M., Kuijpers, A., 2012. Climate variability in West Greenland during the past 1500 years: evidence from a high-resolution marine palynological record from Disko Bay. Boreas 41, 68–83.
Rigor, I.G., Wallace, J.M., Colony, R.L., 2002. Response of sea ice to the Arctic oscillation. J. Clim. 15, 2648–2663.
Rind, D., 2002. The Sun's role in climate variations. Science 296, 673–677.
Roeckner, E., Bäuml, G., Bonaventura, L., Brokopf, R., Esch, M., Giorgetta, M., Hagemann, S., Kirchner, I., Kornblueh, L., Manzini, E., Rhodin, A., Schlese, U., Schulzweida, U., Tompkins, A., 2003. The Atmospheric General Circulation Model ECHAM5. Part 1. Model Description. Report No. 349. Max-Planck-Institut für Meteorologie, Hamburg, Germany.
Roncaglia, L., Kuijpers, A., 2004. Palynofacies analysis and organic-walled dinoflagellate cysts in late-Holocene sediments from Igaliku Fjord, South Greenland. Holocene 14, 172–184.
Ruzmaikin, A., Feynman, J., Jiang, X., Noone, D.C., Waple, A.M., Yung, Y.L., 2004. The pattern of northern hemisphere surface air temperature during prolonged periods of low solar output. Geophys. Res. Lett. 31, L12201.
Schmith, T., Hansen, C., 2003. Fram Strait Ice Export during the Nineteenth and Twentieth Centuries reconstructed from a Multiyear Sea Ice Index from Southwestern Greenland. J. Clim. 16, 2782–2791.
Schröder, W., 2005. Case Studies on the Spörer, Maunder, and Dalton Minima. Science Edition, Bremen.
Schulz, M., Mudelsee, M., 2002. REDFIT: estimating red-noise spectra directly from unevenly spaced paleoclimatic time series. Comput. Geosci. 28, 421–426.
Sedláček, J., Mysak, L., 2009. Sensitivity of sea ice to wind-stress and radiative forcing since 1500: a model study of the Little Ice Age and beyond. Clim. Dyn. 32, 817–831.
Seidenkrantz, M.-S., Aagaard-Sørensen, S., Sulsbrück, H., Kuijpers, A., Jensen, K.G., Kunzendorf, H., 2007. Hydrography and climate of the last 4400 years in a SW Greenland fjord: implications for Labrador Sea palaeoceanography. Holocene 17, 387–401.
Seidenkrantz, M.-S., Roncaglia, L., Fischel, A., Heilmann-Clausen, C., Kuijpers, A., Moros, M., 2008. Variable North Atlantic climate seesaw patterns documented by a late Holocene marine record from Disko Bugt, West Greenland. Mar.

Micropaleontol. 68, 66–83.
Sejrup, H.P., Lehman, S.J., Haflidason, H., Noone, D., Muscheler, R., Berstad, I.M., Andrews, J.T., 2010. Response of Norwegian Sea temperature to solar forcing since 1000 A.D. J. Geophys. Res. 115, C12034.
Sha, L., Jiang, H., Knudsen, K.L., 2012. Diatom evidence of climatic change in Holsteinsborg Dyb, west of Greenland, during the last 1200 years. Holocene 22, 347–358.
Sha, L., Jiang, H., Seidenkrantz, M.-S., Knudsen, K.L., Olsen, J., Kuijpers, A., Liu, Y., 2014. A diatom-based sea-ice reconstruction for the Vaigat Strait (Disko Bugt, West Greenland) over the last 5000 yr. Palaeogeogr. Palaeoclimatol. Palaeoecol. 403, 66–79.
Shindell, D., Rind, D., Balachandran, N., Lean, J., Lonergan, P., 1999. Solar cycle variability, ozone, and climate. Science 284, 305–308.
Sicre, M.-A., Jacob, J., Ezat, U., Rousse, S., Kissel, C., Yiou, P., Eiríksson, J., Knudsen, K.L., Jansen, E., Turon, J.-L., 2008. Decadal variability of sea surface temperatures off North Iceland over the last 2000 years. Earth Planet. Sci. Lett. 268, 137–142.
Sicre, M.-A., Weckström, K., Seidenkrantz, M.S., Kuijpers, A., Benetti, M., Masse, G., Ezat, U., Schmidt, S., Bouloubassi, I., Olsen, J., Khodri, M., Mignot, J., 2014. Labrador current variability over the last 2000 years. Earth Planet. Sci. Lett. 400, 26–32.
Stein, R., Fahl, K., Müller, J., 2012. Proxy reconstruction of Cenozoic Arctic ocean sea-ice history: from IRD to IP25. Polarforschung 82, 37–71.
Steinhilber, F., Abreu, J.A., Beer, J., Brunner, I., Christl, M., Fischer, H., Heikkilä, U., Kubik, P.W., Mann, M., McCracken, K.G., Miller, H., Miyahara, H., Oerter, H., Wilhelms, F., 2012. 9,400 years of cosmic radiation and solar activity from ice cores and tree rings. Proc. Natl. Acad. Sci. U. S. A. 109, 5967–5971.
Stepanek, C., Lohmann, G., 2012. Modelling mid-Pliocene climate with COSMOS. Geosci. Model. Dev. 5, 1221–1243.
Trouet, V., Esper, J., Graham, N.E., Baker, A., Scourse, J.D., Frank, D.C., 2009. Persistent positive North Atlantic oscillation mode dominated the medieval climate anomaly. Science 324, 78–80.
Trouet, V., Scourse, J.D., Raible, C.C., 2012. North Atlantic storminess and Atlantic Meridional Overturning Circulation during the last Millennium: reconciling contradictory proxy records of NAO variability. Glob. Planet. Change 84–85, 48–55.
Varma, V., Prange, M., Merkel, U., Kleinen, T., Lohmann, G., Pfeiffer, M., Renssen, H., Wagner, A., Wagner, S., Schulz, M., 2012. Holocene evolution of the Southern Hemisphere westerly winds in transient simulations with global climate models. Clim. Past 8, 391–402.
Verschuren, D., Laird, K.R., Cumming, B.F., 2000. Rainfall and drought in equatorial east Africa during the past 1,100 years. Nature 403, 410–414.
Vinther, B.M., Buchardt, S.L., Clausen, H.B., Dahl-Jensen, D., Johnsen, S.J., Fisher, D.A., Koerner, R.M., Raynaud, D., Lipenkov, V., Andersen, K.K., Blunier, T., Rasmussen, S.O., Steffensen, J.P., Svensson, A.M., 2009. Holocene thinning of the Greenland ice sheet. Nature 461, 385–388.
Weckström, K., Massé, G., Collins, L.G., Hanhijärvi, S., Bouloubassi, I., Sicre, M.-A., Seidenkrantz, M.-S., Schmidt, S., Andersen, T.J., Andersen, M.L., Hill, B., Kuijpers, A., 2013. Evaluation of the sea ice proxy IP25 against observational and diatom proxy data in the SW Labrador Sea. Quat. Sci. Rev. 79, 53–62.
Wei, W., Lohmann, G., 2012. Simulated Atlantic multidecadal oscillation during the Holocene. J. Clim. 25, 6989–7002.
Wei, W., Lohmann, G., Dima, M., 2012. Distinct modes of internal variability in the global meridional overturning circulation associated with the Southern Hemisphere Westerly Winds. J. Phys. Oceanogr. 42, 785–801.
Werner, K., Spielhagen, R.F., Bauch, D., Hass, H.C., Kandiano, E., Zamelczyk, K., 2011. Atlantic water advection to the eastern Fram Strait — multiproxy evidence for late Holocene variability. Palaeogeogr. Palaeoclimatol. Palaeoecol. 308, 264–276.
Zhang, X., Lohmann, G., Knorr, G., Purcell, C., 2014. Abrupt glacial climate shifts controlled by ice sheet changes. Nature 512, 290–294.
Zhang, X., Lohmann, G., Knorr, G., Xu, X., 2013. Different ocean states and transient characteristics in Last Glacial Maximum simulations and implications for deglaciation. Clim. Past 9, 2319–2333.